Research Paper

A numerical approach based on Bernoulli wavelets for fractional electrical circuits

R.Aruldoss and R. Anusuya Devi

(Department of Mathematics, Government Arts College (Autonomous),(Affiliated to Bharathidasan University, Tiruchirappalli), Kumbakonam, Tamil Nadu, India)
Corresponding Author: R. Anusuya Devi

ABSTRACT: *This article addresses a numerical approach based on Bernoulli wavelets for fractional electrical circuits, namely LC, RL, RC and RLC. The comparative analysis of numerical simulation of each circuit with its classical solution is also discussed.*
KEYWORDS: *Fractional electrical circuits, Bernoulli wavelet, Operational matrix*

I.   INTRODUCTION

Fractional Calculus is centuries-old mathematical subject that involves the integration and differentiation of arbitrary orders. It is the generalization of the classical calculus. However, applications of Fractional Calculus have just recently developed in numerous fields of physics, chemistry, engineering, finance and social sciences [11].

Most of the fractional differential equations do not have analytical solutions. Besides numerical approaches, some approximate methods such as separation of variables [14], Variational iteration method [15], Adomian decomposition method [10], Homotopy analysis method [4], Homotopy perturbation method [7] and Finite difference method [8] are relatively new approaches to provide an analytical approximation to fractional differential equations.

Recently, wavelet analysis has considerable attention in solving fractional differential equations. Wavelets have applications in signal analysis, image compression, medical science and many other areas.

Here, we analyze the following different types of fractional electrical circuits, namely LC(Inductor-Capacitor) circuit, RL(Resistor-Inductor) circuit, RC(Resistor-Capacitor) circuit and RLC(Resistor-Inductor-Capacitor).

Fractional models for electrical circuits have already been proposed [6]. In this regard, Gomez et al. [1] have obtained solutions of RL and RC circuits involving caputo derivatives using numerical Laplace transform. Besides, they have also studied RLC circuit in time domain and found solution with respect to the Mittag-Leffler function. Shah et al. [13] considered the Laplace transform of fractional derivatives in the caputo sense to get the solutions of RL electrical circuit described by a fractional differential equation of the order $0<\beta\leq1$.

Atangana et al. [3] examined RLC circuit model via the fractional derivative without singular kernel. To study fractional electrical circuits, Legendre wavelet has been applied by Arora and Chauhan [2]. Recently, Sahar Altaf and Sumaira Yousuf Khan have found the numerical solutions of electrical circuits described by fractional derivatives [12].

The outline of this paper is as follows: In section 2, we discuss some basic definitions. In section 3, we present Bernoulli wavelets and their properties. In section 4, we discuss the function approximation and derive operational matrix of fractional integration. We discuss four fractional electrical circuit equations to illustrate the applicability of the proposed method and compare the results with the classical solutions in section 5. Finally, conclusion is given in section 6.

II.   PRELIMINARY CONCEPTS

In this section, some basic definitions and preliminaries of fractional calculus are presented.

Definition 2.1. The Riemann-Liouville fractional integral operator I^γ of order $\gamma \geq 0$ is defined as

$$(I^\gamma g)(x) = \begin{cases} \dfrac{1}{\Gamma(\gamma)} \displaystyle\int_0^x (x-\tau)^{\gamma-1} g(\tau) d\tau, & \gamma > 0 \\ g(x), & \gamma = 0 \end{cases} \tag{2.1}$$

where $g(x) \epsilon L^1(\mathbb{R}^+)$ and Riemann-Liouville fractional derivative operator D_{RL}^γ is defined by

$$(D_{RL}^\gamma g)(x) = \left(\frac{d}{dx}\right)^n (I^{n-\gamma} g)(x), \qquad n-1 < \gamma \leq n, \ n \epsilon \mathbb{N}$$

where $g(x) \epsilon L^1(\mathbb{R}^+)$.

Some properties of I^γ are listed below.

$$I^\alpha \left(I^\beta g(x) \right) = I^\beta \left(I^\alpha g(x) \right) = I^{\alpha+\beta} g(x), \tag{2.2}$$

$$I^\alpha (x-\alpha)^\gamma = \frac{\Gamma(\gamma+1)}{\Gamma(\alpha+\gamma+1)} (x-\alpha)^{\alpha+\gamma}, \tag{2.3}$$

where $\alpha, \beta \geq 0$ and $\gamma > -1$.

Definition 2.2. The Caputo fractional derivative operator of order $\gamma \geq 0$ is defined as

$$(D^\gamma g)(x) = \begin{cases} g^{(n)}(x), & \gamma = n \epsilon \mathbb{N} \\ \dfrac{1}{\Gamma(n-\gamma)} \displaystyle\int_0^x \frac{g^n(\tau)}{(x-\tau)^{\gamma+1-n}} d\tau, & n-1 < \gamma < n, \end{cases} \tag{2.4}$$

where $g(x) \epsilon L^1(\mathbb{R}^+)$.

The relations between the Riemann-Liouville operator and the Caputo operator are given by the following expressions.

$$(D^\gamma I^\gamma g)(x) = g(x)$$

and

$$(I^\gamma D^\gamma g)(x) = g(x) - \sum_{k=0}^{n-1} g^{(k)}(0^+) \frac{x^k}{k!}, \qquad n-1 < \gamma \leq n, \tag{2.5}$$

where $n \epsilon \mathbb{N}$ and $g^{(k)}(0^+) := lim_{x \to 0^+} D^k g(x)$, $\qquad k = 0,1,2,\dots,n-1$.

III.   BERNOULLI WAVELETS

Wavelets consist of a family of functions generated from dilations and translations of a single function $\psi(x)$, called the mother wavelet. If the dilation parameter c and the translation parameter d change continuously, we obtain the following continuous family of wavelets,

$$\psi_{c,d}(x) = |c|^{-\frac{1}{2}} \psi\left(\frac{t-d}{c}\right), \ c \neq 0, d \in \mathbb{R}.$$

If the translation and dilation parameters are chosen to have discrete values, that is, $c = c_0^{-l}$, $d = nd_0 c_0^{-l}$, $c_0 > 1$, $d_0 > 0$ and $l, n \in \mathbb{N}$, we have the following family of discrete wavelets,

$$\psi_{ln}(x) = |c_0|^{\frac{1}{2}} \psi(c_0^l x - nd_0),$$

where $\{\psi_{ln}\}$ forms a basis for $L^2(\mathbb{R})$. In particular, if $c_0 = 2$ and $d_0 = 1$, we can obtain orthonormal basis from $\{\psi_{ln}\}$ for $L^2(\mathbb{R})$.

The Bernoulli wavelets for $x \in [0,1)$ are defined as

$$\psi_{pq}(x) = \begin{cases} 2^{\frac{u-1}{2}} \widetilde{W}_q (2^{u-1} x - p + 1), & \frac{p-1}{2^{u-1}} \leq x < \frac{p}{2^{u-1}}, \\ 0, & otherwise, \end{cases} \tag{3.1}$$

for $p = 1,2,\dots,2^{u-1}, q = 0,1,\dots,Q-1$ and $u, Q \in \mathbb{N}$, where

$$\widetilde{W}_q(x) = \begin{cases} 1, & q = 0, \\ \dfrac{1}{\sqrt{\dfrac{(-1)^{q-1}(q!)^2}{(2q)!}\gamma_{2q}}} W_q(x), & q > 0, \end{cases}$$

the dilation parameter is $2^{-(u-1)}$, the translation parameter $(p-1)2^{-(u-1)}$, and the coefficient $\dfrac{1}{\sqrt{\dfrac{(-1)^{q-1}(q!)^2}{(2q)!}\gamma_{2q}}}$ is used for orthonormal condition. Here $W_q(x), q = 0,1,\dots,Q-1$, denote Bernoulli polynomials of order q.

3.1 Function approximation

A function $h(x = L^2[0,1))$ can be expanded as

$$h(x) = \sum_{p=0}^{\infty} \sum_{q\in\mathbb{Z}} a_{pq}\psi_{pq}(x) \tag{3.2}$$

where the coefficients a_{pq} are given by

$$a_{pq} = <h(x),\psi_{pq}(x)> = \int_0^1 h(x)\,\psi_{pq}(x)dx.$$

If the infinite series in equation (3.2) is truncated, then it can be written as

$$\widetilde{h(x)} \approx \sum_{p=1}^{2^{u-1}} \sum_{q=0}^{Q-1} a_{pq}\,\psi_{pq}(x). \tag{3.3}$$

For simplicity, equation (3.3) is written as

$$\widetilde{h(x)} = \sum_{i=1}^{q'} a_i\,\psi_i(x) = A^T\Psi(x), \tag{3.4}$$

where $a_i = a_{pq}, \psi_i = \psi_{pq}, q' = 2^{u-1}Q, A = [a_1, a_2, \dots, a_{q'}]^T$, $\tag{3.5}$
$\Psi(x) = [\psi_1(x), \psi_2(x), \dots, \psi_{q'}(x),]^T$ and $\tag{3.6}$
the index i is determined by the relation $i = Q(p-1) + q + 1$.

We define the Bernoulli wavelet coefficient matrix $\phi_{q'\times q'}$, $q' = 2^{u-1}Q$, at the collocation points $x_r = \dfrac{2r-1}{2q'}, r = 1,2,\dots,q'$ as

$$\phi_{q'\times q'} = \left[\Psi\left(\frac{1}{2q'}\right), \Psi\left(\frac{3}{2q'}\right), \dots, \Psi\left(\frac{2q'-1}{2q'}\right)\right]. \tag{3.7}$$

Specifically, the Bernoulli wavelet coefficient matrix for $u = 2$ and $Q = 3$ becomes

$$\phi_{6\times 6} = \begin{pmatrix} 1.4142 & 1.4142 & 1.4142 & 0 & 0 & 0 \\ -1.6330 & 0 & 1.6330 & 0 & 0 & 0 \\ 0.5270 & -1.5811 & 0.5270 & 0 & 0 & 0 \\ 0 & 0 & 0 & 1.4142 & 1.4142 & 1.4142 \\ 0 & 0 & 0 & -1.6330 & 0 & 1.6330 \\ 0 & 0 & 0 & 0.5270 & -1.5811 & 0.5270 \end{pmatrix} \tag{3.8}$$

Here, we have

$$\widetilde{h_{q'}} = \left[\tilde{h}(x_1), \tilde{h}(x_2), \dots, \tilde{h}(x_{q'})\right] = A^T\phi_{q'\times q'}.$$

Since the Bernoulli wavelet coefficient matrix $\phi_{q'\times q'}$ is invertible, it is possible to obtain the Bernoulli wavelet coefficient vector A^T by $\widetilde{h_{q'}}\phi_{q'\times q'}^{-1}$.

3.2 Operational matrix of fractional order integration

In this section, we explore the basic idea of finding the operational matrix of fractional order integration for the Bernoulli wavelets.

On $[0,1)$, we define q'- set series of Block pulse functions (BPFs) as

$$b_r(x) = \begin{cases} 1, & (r-1)/q' \le x < r/q', \\ 0, & otherwise \end{cases} \tag{3.9}$$

where $r = 1,2,3,\dots,q'$. For $x \in [0,1)$, $h(x) \in L^2[0,1)$ can be approximated by using BPFs as

$$h(x) \simeq \sum_{r=1}^{q'} h_r \, b_r(x) = h^T B_{q'}(x), \tag{3.10}$$

where $h = [h_1, h_2, \ldots, h_{q'}]^T$, h_r for $r = 1,2, \ldots, q'$ are given by

$$h_r = \frac{1}{q'} \int_{(r-1)/q'}^{r/q'} h(x) b_r(x) dx.$$

Bernoulli wavelets can be expanded into q'-term BPFs as

$$\Psi(x) = \phi_{q' \times q'} B_{q'}(x), \tag{3.11}$$

where $B_{q'}(x) = [b_1(x), \, b_2(x), \ldots, b_{q'}(x)]^T$.

The block pulse operational matrix $H^\beta, \beta \geq 0$ of fractional integration of order $\beta \geq 0$ is defined as [9],

$$(I^\beta B_{q'})(x) \approx H^\beta B_{q'}(x), \tag{3.12}$$

where

$$H^\beta = \frac{1}{q'^\beta} \frac{1}{\Gamma(\beta + 2)} \begin{pmatrix} 1 & \zeta_1 & \zeta_2 & \zeta_3 & \cdots & \zeta_{q'-1} \\ 0 & 1 & \zeta_1 & \zeta_2 & \cdots & \zeta_{q'-2} \\ 0 & 0 & 1 & \zeta_1 & \cdots & \zeta_{q'-3} \\ \vdots & \vdots & \ddots & \ddots & \vdots & \vdots \\ 0 & 0 & \cdots & 0 & 1 & \zeta_1 \\ 0 & 0 & \cdots & 0 & 0 & 1 \end{pmatrix},$$

with $\zeta_u = (u+1)^{\beta+1} - 2u^{\beta+1} + (u-1)^{\beta+1}$.

The fractional integration of Bernoulli wavelets can be expanded as

$$(I^\beta \Psi)(x) \approx P_{q' \times q'}^\beta \Psi(x), \tag{3.13}$$

where $P_{q' \times q'}^\beta$ is operational matrix of fractional integration of order $\beta \geq 0$ based on the Bernoulli wavelets.

From Equations (3.12) and (3.13), we have

$$(I^\beta \Psi)(x) \approx (I^\beta \phi_{q' \times q'} B_{q'})(x) = \phi_{q' \times q'} (I^\beta B_{q'})(x) \approx \phi_{q' \times q'} H^\beta B_{q'}(x). \tag{3.14}$$

Thus combining Equations (3.13) and (3.14), we attain

$$P_{q' \times q'}^\beta \Psi(x) \approx (I^\beta \Psi)(x) \approx \phi_{q' \times q'} H^\beta B_{q'}(x) = \phi_{q' \times q'} H^\beta \phi_{q' \times q'}^{-1} \Psi(x), \text{ and so} \tag{3.15}$$

$$P_{q' \times q'}^\beta \approx \phi_{q' \times q'} H^\beta \phi_{q' \times q'}^{-1}. \tag{3.16}$$

For example, letting $u = 2, Q = 3$, and $\beta = 0.5$, the operational matrix $P_{q' \times q'}^\beta$ becomes

$$P_{6 \times 6}^{0.5} = \begin{pmatrix} 0.5282 & 0.1819 & -0.0298 & 0.4438 & -0.0871 & 0.0256 \\ -0.1452 & 0.2243 & 0.1329 & 0.0799 & -0.0449 & 0.0198 \\ -0.0598 & -0.0964 & 0.1688 & -0.0417 & -1.8589e - 04 & 0.0029 \\ 0 & 0 & 0 & 0.5282 & 0.1819 & -0.0298 \\ 0 & 0 & 0 & -1.1452 & 0.2243 & 0.1329 \\ 0 & 0 & 0 & -0.0598 & -0.0964 & 0.1688 \end{pmatrix} \tag{3.17}$$

Since the operational matrix $P_{6 \times 6}^{0.5}$ contains several zeros, the proposed technique reduces the computation greatly.

IV. APPLICATIONS

This section deals with the applicability and the simplicity of the proposed technique in solving fractional differential equations of the electrical circuits LC, RL, RC and RLC.

4.1 LC Circuit
Consider the fractional differential equation of an LC Circuit with charged capacitor and inductor,

$$D^\beta R(t) + \rho_0^2 R(t) = 0, \qquad \beta \epsilon [1,2], \text{ where } \rho_0^2 = \frac{1}{LC} \tag{4.1}$$

with $R(0) = R_0$ and $R'(0) = 0$.

The classical solution for $\beta = 2$ is $R(t)_{LC} = R_0 \cos(\rho_0 t)$. \hfill (4.2)

Table 1: Numerical results of LC circuit (L=1,C=1,$R_0 = 0.01$ and for $\beta = 2$)

t	u=2,Q=2	u=3,Q=2	u=4,Q=2	CS
1/16	1.0050×10^{-3}	9.9740×10^{-3}	9.9740×10^{-3}	9.9805×10^{-3}
3/16	9.7439×10^{-3}	9.8186×10^{-3}	9.8184×10^{-3}	9.8247×10^{-3}
5/16	9.4378×10^{-3}	9.5101×10^{-3}	9.5096×10^{-3}	9.5157×10^{-3}
7/16	9.1317×10^{-3}	9.0535×10^{-3}	9.0525×10^{-3}	9.0581×10^{-3}
9/16	8.5201×10^{-3}	8.4557×10^{-3}	8.4542×10^{-3}	8.4592×10^{-3}
11/16	7.6764×10^{-3}	7.7262×10^{-3}	7.7240×10^{-3}	7.7283×10^{-3}
13/16	6.8327×10^{-3}	6.8762×10^{-3}	6.8733×10^{-3}	6.8769×10^{-3}
15/16	5.9890×10^{-3}	5.9191×10^{-3}	5.9154×10^{-3}	5.9181×10^{-3}

Approximating $D^\beta R(t)$ as $C^T\psi(t)$, we have (4.3)

$R(t) = C^T P^\beta \psi(t) + tR'(0) + R(0)$ (4.4)

Using the initial conditions, $R(t) = C^T P^\beta \psi(t) + R_0$ (4.5)

Thus $C^T\psi(t) + \rho_0^2\left[C^T P^\beta \psi(t) + R_0\right] = 0$ (4.6)
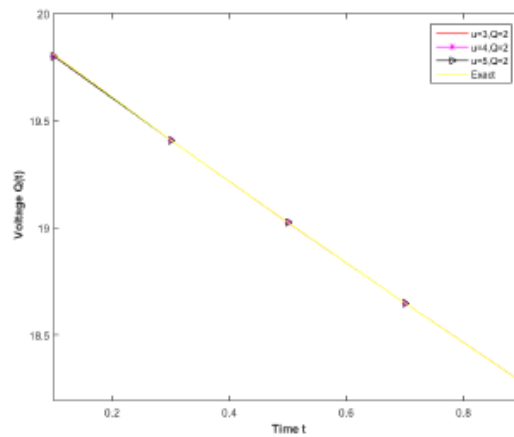

Figure 1: Current versus Time graph (L=1, C=1, $R_0 = 0.01\ and\ \beta = 2$)

Solving the equation (4.6) at the collocation points, we get the Bernoulli coefficient vector C^T. The numerical solutions of the LC circuit for $\beta = 2$ and various values of q' are given in Table 1. Also, from Fig 1, it is graphically shown that the proposed Bernoulli wavelet based numerical approach reaches a higher precision of accuracy.

4.2 RL Circuit

Consider the fractional differential equation of an RL Circuit with only charged capacitor and resistor

$D^\beta Q(t) + \kappa Q(t) = \rho, \qquad \beta \epsilon (0,1],$ (4.7)

with the initial state $Q(0) = Q_0$ where $\kappa = \frac{R}{L}, \rho = \frac{V}{L}$

The classical solution for $\beta = 1$ is

$Q(t) = \left[Q_0 - \frac{VL}{R}\right]e^{-\kappa t} + \frac{VL}{R}$ (4.8)

Table 2: Numerical results of RL circuit (R=10, L=1, $Q_0 = 0.01$, $V = 10$ and for $\beta = 1$)

t	u=2,Q=2	u=3,Q=2	u=4,Q=2	CS
1/16	4.3778×10^{-1}	3.9077×10^{-1}	4.2531×10^{-1}	4.7009×10^{-1}
3/16	6.8222×10^{-1}	8.5941×10^{-1}	8.423×10^{-1}	8.4818×10^{-1}
5/16	9.2667×10^{-1}	9.6756×10^{-1}	9.5674×10^{-1}	9.5650×10^{-1}
7/16	11.7111	9.9251×10^{-1}	9.8813×10^{-1}	9.8754×10^{-1}
9/16	9.9306×10^{-1}	9.9827×10^{-1}	9.9674×10^{-1}	9.9643×10^{-1}
11/16	9.9607×10^{-1}	9.9960×10^{-1}	9.9911×10^{-1}	9.9898×10^{-1}
13/16	9.9909×10^{-1}	9.9991×10^{-1}	9.9975×10^{-1}	9.9971×10^{-1}
15/16	10.0212	9.9998×10^{-1}	9.9993×10^{-1}	9.9992×10^{-1}

Approximating $D^\beta Q(t)$ as $C^T \psi(t)$, we have (4.9)

$Q(t) = C^T P^\beta \psi(t) + Q(0)$ (4.10)

Using the initial conditions, we attain

$Q(t) = C^T P^\beta \psi(t) + Q_0$ (4.11)

Thus $C^T \psi(t) + \kappa [C^T P^\beta \psi(t) + Q_0] = \rho$ (4.12)

By solving the above matrix equation at the collocation points, we obtain Bernoulli coefficient vector C^T. The Table 2 shows the numerical solutions of the RL circuit for $\beta = 1$ and various values of q'. As it is clearly seen in Fig. 2, the graphical behavior of the fractional RL circuit is similar to the classical solution for $\beta = 1$.
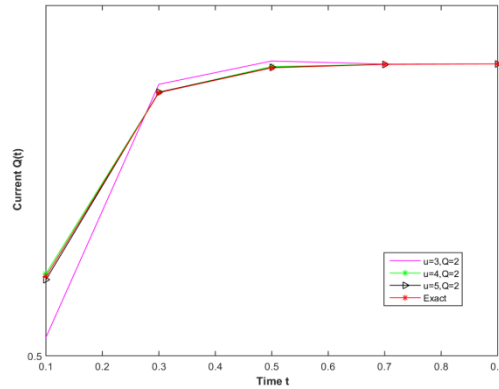

Figure 2: Current versus Time graph (R=10, L=1, $Q_0 = 0.01$, V=10 and $\beta = 1$)

4.3 RC Circuit

Consider the fractional differential equation of an RC Circuit with resistance and charged capacitance

$D^\beta Q(t) + \mu Q^\beta(t) = 0, \qquad \beta \epsilon [0,1]$ (4.13)

with the condition $Q(0) = Q_0$, where $\mu = \frac{1}{RC}$.

The classical solution for $\beta = 1$ is $Q(t) = Q_0 e^{-\mu t}$ (4.14)

Table 3: Numerical results of RC circuit (R=10, C=1, $Q_0 = 20$ and for $\beta = 1$)

t	u=3,Q=2	u=4,Q=2	u=5,Q=2	CS
1/16	19.8758	19.8756	19.8753	19.8754
3/16	19.6289	19.6287	19.6284	19.6285
5/16	19.3850	19.3849	19.3846	19.3847
7/16	19.1443	19.1440	19.1438	19.1439
9/16	18.9064	18.9062	18.9060	18.9061
11/16	18.6715	18.6714	18.6711	18.6712
13/16	18.4396	18.4394	18.4392	18.4394
15/16	18.2105	18.2104	18.2102	18.2102

Approximating $D^\beta Q(t)$ as $C^T \psi(t)$, we have (4.15)

$Q(t) = C^T P^\beta \psi(t) + Q(0)$ (4.16)

Using the initial condition, we attain

$Q(t) = C^T P^\beta \psi(t) + Q_0$ (4.17)

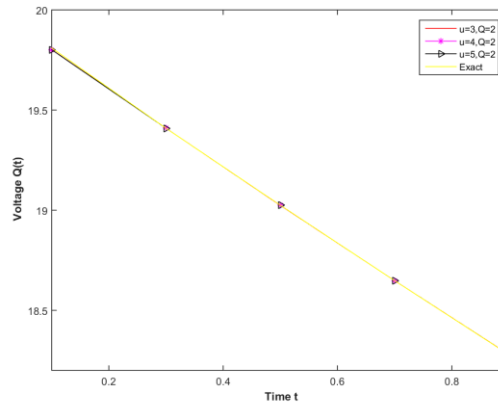Thus $C^T \psi(t) + \mu [C^T P^\beta \psi(t) + Q_0] = 0$ (4.18)

Figure 3: Voltage versus Time graph (R=10, C=1, $Q_0 = 20, \beta = 1$)

Solving this system at the collocation points, we obtain Bernoulli coefficient vector C^T. The numerical solutions of the RC Circuit for $\beta = 1$ and different values of q' are given in the Table 3. Also graphical analysis for different values of q' is shown in Fig.3. As it is seen in Fig 3, the graphical behavior of fractional RC circuit is close to the classical solution for $\beta = 1$.

4.4 RLC Circuit

Consider the fractional differential equation of an RLC Circuit with resistance, inductance and charged capacitance

$$D^{2\beta}Q(t) + \rho Q^{\beta}(t) + \eta Q(t) = 0, \qquad \beta\epsilon[1/2,1] \tag{4.19}$$

with the conditions $Q(0) = Q_0$ and $Q'(0) = 0$, where $\eta = \frac{1}{LC}$ and $\rho = \frac{R}{L}$.

The classical solution for $\beta = 1$ is

$$Q(t) = \frac{Q_0}{k_1 - k_2}[-k_2 e^{k_1 t} + k_1 e^{k_2 t}], \tag{4.20}$$

where $k_1 = \frac{-\rho + \sqrt{\rho^2 - 4\eta}}{2}, k_2 = \frac{-\rho - \sqrt{\rho^2 - 4\eta}}{2}$

Table 4: Numerical results of RLC circuit (R=10, L=10, C=10, $Q_0 = 0.01$ and for $\beta = 1$)

t	u=2,Q=2	u=3,Q=2	u=4,Q=2	CS
0.1	0.01096	0.01093	0.01095	0.0099991
0.2	0.01174	0.01181	0.0118	0.0099981
0.3	0.01253	0.01259	0.01259	0.0099959
0.4	0.01331	0.01328	0.01329	0.0099930
0.5	0.01409	0.01396	0.01393	0.0009989
0.6	0.01451	0.01449	0.01450	0.0099953
0.7	0.01498	0.01502	0.01501	0.010006
0.8	0.01545	0.01548	0.01547	0.010005
0.9	0.01592	0.01589	0.01590	0.010009

Approximating $D^{2\beta}Q(t)$ as $C^T\psi(t)$, we have (4.21)

$$D^{\beta}Q(t) = C^T P^{\beta}\psi(t) + Q(0) \tag{4.22}$$

$$Q(t) = C^T P^{2\beta}\psi(t) + Q(0)\frac{t^{\beta}}{\Gamma(\beta+1)} + Q_0 \tag{4.23}$$

Thus $C^T\psi(t) + \rho\left[C^T P^\beta \psi(t) + Q_0\right] + \eta\left[C^T P^{2\beta}\psi(t) + Q(0)\frac{t^\beta}{\Gamma(\beta+1)} + Q_0\right] = 0$ (4.24)
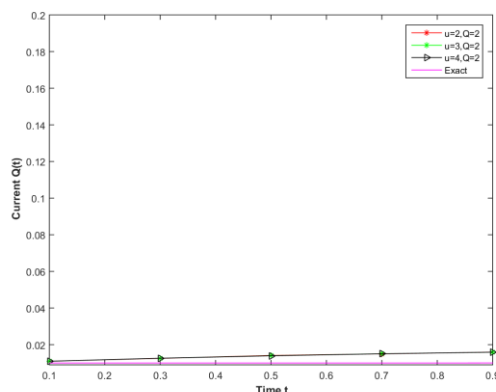

Figure 4: Current versus Time graph (R=10, L=10, C=10, $Q_0 = 0.01$ and $\beta = 1$)

Solving the equation (4.24) at the collocation points, we obtain Bernoulli coefficient vector C^T. The numerical solutions of the RLC circuit for $\beta = 1$ and different values q' are given in the Table 4. Also the graphical analysis for different values of q' is shown in Fig.4. As it is seen in Fig.4, the graphical behavior of fractional RLC circuit is close to the classical solution for $\beta = 1$.

IV. CONCLUSION

The proposed numerical technique based on Bernoulli wavelets is employed to find the approximate solutions of fractional electrical circuit models namely, LC, RL, RC and RLC. The graphs in Figures(1-4) represent the numerical solutions of such models which behave similar to the classical solutions. Thus the proposed method gives the fast convergence to the solutions and so can be further applied to other physical models in real-life problems.

REFERENCES

[1]. A.Alsaedi, J.J.Nieto, V.Venktesh., Fractional electrical circuits, Advances in Mechanical Engineering, 2015,7(11).
[2]. R.Arora, N.S.Chauhan., An application of Legendre wavelet in fractional electrical circuits, Global Journal of Pure and Applied mathematics, 2017, 13(2):183-202.
[3]. A. Atangana, J.J.Nieto, Numerical solution for the model of RLC Circuit via the fractional derivative without singular kernel, Advances in Mechanical Engineering, 2015.
[4]. A. Demir , MA Bayrak , E.Ozbilge, A new approach for the approximate analytic solution of space-time fractional differential equations by the homotopy analysis method, Adv Math Phys (2019).
[5]. R.Garrappa, M.Popolizio, On the use of matrix functions for fractional partial differential equations, Math.Comput.Simulation 81(2011) 1045-1056.
[6]. J.F.Gomez, C.M. Astorga, R.F. Escobas, M.A.Medina, R.Gauzman, A.Gonzaleg and D.Baleanu, Overview of simulation of fractional differential equation using numerical Laplace transform, Cent. Eur.J.Phys.(CEJP) 2012; 1-14.
[7]. S.Javeed , D.Baleanu , A.Waheed , M.Shaukat Khan , H.Affan, , Analysis of homotopy perturbation method for solving fractional order differential equations, Mathematics 7(1):40, (2019).
[8]. G.Karamali, M.Dehghan, M.Abbaszadeh, Numerical solution of time-fractional partial differential equation in the electro-analytical chemistry by a local meshless method, Eng Comput 35(1): 87-100, (2019).
[9]. A.Kilicman, Kronecker operational matrices for fractional calculus and some applications, Appl Math Comput 187:250-265.
[10]. W.Li , Y.Pang, Application of Adomian decomposition method to nonlinear systems, Adv Differ Equ 2020:67.
[11]. I.Podlubny, Fractional Differential Equations, in: Mathematics in Science and Engineering, Vol.198, Academic Press Inc, San Diego, CA, 1999.
[12]. Sahar Altaf, Sumaira Yousuf Khan, Numerical solution of fractional electrical circuits by Haar wavelet, Matematika: MJIAM, 2019, Volume 35, Number 3, 331-343.
[13]. P.V.Shah, A.D.Patel, I.A.salehbhai and A.K.Shukla, Analytic solution for the RL electric circuit model in fractional order, Abstract and applied analysis, 2014.
[14]. S.Shen,F. Liu, VV.Anh, The analytical solution and numerical solutions for a two-dimensional multi-term time fractional diffusion and diffusion-wave equation, J Comput Appl Math 345:515-534, (2019).
[15]. D.Ziane, MH.Cherif, Variational iteration transform method for fractional differential equations, J.Interdiscip Math 21(1): 185-199, (2018).